Check for updates

METHOD ARTICLE

REVISED **Non-Invasive measurement of the cerebral metabolic rate of oxygen using MRI in rodents** [version 4; peer review: 2 approved]

Tobias C Wood (iD), Diana Cash, Eilidh MacNicol (iD), Camilla Simmons (iD), Eugene Kim (iD), David J Lythgoe, Fernando Zelaya, Federico Turkheimer (iD)

Department of Neuroimaging, Institute of Psychiatry, Psychology & Neuroscience, King's College London, SE5 8AF, UK

Abstract

Malfunctions of oxygen metabolism are suspected to play a key role in a number of neurological and psychiatric disorders, but this hypothesis cannot be properly investigated without an *in-vivo* non-invasive measurement of brain oxygen consumption. We present a new way to measure the Cerebral Metabolic Rate of Oxygen ($CMRO_2$) by combining two existing magnetic resonance imaging techniques, namely arterial spin-labelling and oxygen extraction fraction mapping. This method was validated by imaging rats under different anaesthetic regimes and was strongly correlated to glucose consumption measured by autoradiography.

Keywords

MRI, CMRO2, CBF, OEF, Glucose, Metabolism

Open Peer Review

Approval Status ✓ ✓

	1	2
version 4 (revision) 25 Aug 2022	✓ view	
version 3 (revision) 11 Jul 2022	? view	
version 2 (revision) 09 Sep 2021	? view	✓ view
version 1 13 May 2021	? view	✓ view

1. **Avery Berman** (iD), Massachusetts General Hospital, Charlestown, USA
   Carleton University, Ottawa, Canada
   The Royal Ottawa Institute of Mental Health Research, Ottawa, Canada

2. **Yolanda Ohene** (iD), The University of Manchester, Manchester, UK

Any reports and responses or comments on the article can be found at the end of the article.

Corresponding author: Tobias C Wood (tobias.wood@kcl.ac.uk)

Author roles: Wood TC: Conceptualization, Data Curation, Formal Analysis, Investigation, Methodology, Project Administration, Software, Visualization, Writing – Original Draft Preparation, Writing – Review & Editing; **Cash D**: Conceptualization, Data Curation, Formal Analysis, Funding Acquisition, Investigation, Methodology, Project Administration, Visualization, Writing – Original Draft Preparation, Writing – Review & Editing; **MacNicol E**: Conceptualization, Investigation, Methodology, Project Administration, Visualization, Writing – Original Draft Preparation, Writing – Review & Editing; **Simmons C**: Investigation, Methodology, Project Administration, Writing – Review & Editing; **Kim E**: Investigation, Methodology, Project Administration, Writing – Review & Editing; **Lythgoe DJ**: Conceptualization, Methodology, Project Administration, Writing – Review & Editing; **Zelaya F**: Conceptualization, Methodology, Project Administration, Supervision, Writing – Review & Editing; **Turkheimer F**: Conceptualization, Funding Acquisition, Methodology, Project Administration, Supervision, Writing – Review & Editing

How to cite this article: Wood TC, Cash D, MacNicol E *et al.* **Non-Invasive measurement of the cerebral metabolic rate of oxygen using MRI in rodents [version 4; peer review: 2 approved]** Wellcome Open Research 2022, **6**:109 https://doi.org/10.12688/wellcomeopenres.16734.4

First published: 13 May 2021, **6**:109 https://doi.org/10.12688/wellcomeopenres.16734.1

Introduction

The brain requires around 20% of a human's energy production, and hence requires a similar proportion of the body's oxygen supply[1,2]. There is great interest in being able to quantitatively map the Cerebral Metabolic Rate of Oxygen (CMRO$_2$) consumption, both as a marker of pathology and for the study of healthy ageing[3–6]. Although methods exist using oxygen isotopes with either Magnetic Resonance (MR) spectroscopic imaging or Positron Emission Tomography (PET)[7–9], it would be advantageous to use proton-based Magnetic Resonance Imaging (MRI) methods due to their low invasiveness, lower cost, and wider availability. Recent years have seen the emergence of methods including whole-brain measurements of CMRO$_2$ using a combination of T2-mapping and phase-contrast velocity measurements[10,11], voxel-wise mapping using quantitative Blood Oxygenation Level Dependent (qBOLD)[12], BOLD calibrated with gas administration[13,14] and high-resolution mapping methods based on Quantitative Susceptibility Mapping (QSM)[12,15].

For this study we implemented a straightforward and robust method to measure CMRO$_2$, which combines measurements of Cerebral Blood Flow (CBF) and Oxygen Extraction Fraction (OEF) made with a pre-clinical MRI scanner. We calculated CBF maps using Arterial Spin Labelling (ASL)[16]. OEF maps were constructed by measuring the reversible rate of transverse relaxation R2′, which is related to the concentration of deoxyhaemoglobin (dHb)[17–19].

We demonstrated our method by imaging rats with two anaesthetics known to affect brain metabolism differently, and compared these MRI measurements to gold-standard auto-radiography measurements of glucose metabolism under the same anaesthetics. Although we found our MRI methods underestimated metabolism, we could still detect a relative effect between anesthetics.

Methods

Ethics statement

Study procedures were conducted in accordance with the Animal (Scientific Procedures) Act 1986 and with ethical approval from the King's College London Animal Welfare And Ethical Review Body (AWERB) under the authorisation of license number P023CC39A. All harm to animals was prevented as procedures were performed under terminal anaesthesia. Animals were group housed under standard laboratory conditions with freely available food and water. There were no exclusion criteria for the animals.

Theory

CMRO$_2$, here measured in µmol/100g/min, is defined as the product of CBF, measured in ml/100g/min, and OEF multiplied by the constant C_a which describes the amount of oxygen carried in arterial blood:

$$CMRO_2 = CBF \times OEF \times C_a \tag{1}$$

Throughout this paper we use a value of C_a=8.48 µmol/ml, calculated from the values for mice given in Gagnon *et al.*[20]. Typical values used for healthy humans are 8.04 and 8.33 µmol/ml[13,21].

The measurement of CBF (measured in ml/100g/min) with ASL is a well-established MR method[16,22]. We chose to measure OEF from R2′, which is defined as the difference between the combined relaxation rate R_2* and the irreversible relaxation rate R_2 (R_2* = R_2 + R_2′), where relaxation rates are the inverses of relaxation times (R_2′ = 1/ T_2′). MR images can be acquired with T_2′-weighting using an Asymmetric Spin-Echo (ASE) sequence where the refocusing pulse is offset from the standard time to produce a spin echo, T_E/2, by an echo-shift τ/2, which can be either positive (the pulse occurs later than T_E/2 or negative (the pulse occurs earlier than T_E/2[18]. Echoes formed at the same T_E but different τ will hence have the same T_2-weighting, but different amounts of additional T_2′ (or R_2′) weighting. By observing the signal in each voxel from multiple τ values, we can measure a mono-exponential R_2′ as we would measure R_2 from multiple values of T_E.

However, in brain tissue the observed signal value at τ = 0 is less than would be expected from extrapolating the signal curve for τ ≠ 0 back to the origin. This discrepancy can be attributed to static dephasing of spins in susceptibility gradients. The principle biological contributor to such gradients is the presence of deoxyhaemoglobin (dHb) in capillaries and draining veins[17]. In preference to the asymptotic equations used by Stone and Blockey[18] we adapt the full qBOLD equation from He and Yablonskiy[23]:

$$S(\tau) = S_0 exp(-DBV \times f_c(\delta\omega \times \tau)) \tag{2}$$

where

$$f_c(\delta\omega \times \tau) = \frac{1}{3}\int_0^1 du(2+u)\sqrt{1-u}\frac{1-J_0(1.5\delta\omega \times \tau \times u)}{u^2}$$

and $\delta\omega$=R_2′/DBV is the characteristic frequency. We have neglected the dependence of S_0 on TE and T_2 for clarity. The OEF can then be found by

$$OEF = \frac{3\delta\omega}{4\pi\gamma B0\delta\chi_0 Hct}$$

where γ =2π × 42.577 MHz is the proton gyro-magnetic ratio, B_0 is the magnetic field strength, $\delta\chi_0$ = 0.264 × 10^{-6} is the susceptibility difference between oxygenated and deoxygenated blood cells, and we used a haematocrit (Hct) value of 0.34[19]. In previous clinical studies it has been possible to estimate

DBV from the ASE data[19]. We found that we could not reliably fit the data for both DBV and OEF at 9.4T and hence we fixed the value of DBV to 3.3% (see discussion)[23].

R2′ is not only affected by deoxygenated blood, but by any source of susceptibility gradients. The principal of these are background or Macroscopic Field Gradients (MFGs) from air/tissue interfaces, which can be corrected with Z-shimming[18,19]. A Z-shim is an additional small gradient played during the spin-echo formation which partially rephases signals in voxels affected by MFGs, but de-phases signal in unaffected voxels[24,25]. By acquiring and combining multiple images with different Z-shims, the lost signal from MFGs can be restored across the whole image, but will not affect the signal from sub-voxel susceptibility gradients due to deoxygenated blood[19]. In the human brain the largest MFGs are present above the nasal sinus, where air is closest to the parenchyma, and hence the largest susceptibility gradient exists in the Z (axial, in humans superior-inferior) direction. In rodents, the largest voids within the head are the mastoids, and in addition the skull and the tissue surrounding the brain are significantly thinner than in humans. We hence found that gradients in the Y (in animals the superior-inferior) direction were also a significant issue and so added shimming in both the Z and Y directions.

Imaging protocol
A total of ten adult male healthy Sprague-Dawley rats (440–537 g; Charles River) were imaged in a 9.4 Tesla pre-clinical MR system using a four-channel head receive coil, transmit body coil and separate ASL labelling coil (Bruker GmbH). All rats were initially anaesthetised by inhaling 5% isoflurane in an 80:20 mix of air and medical oxygen. Five of the rats were maintained with 2.5% isoflurane for the duration of scanning, while the remaining five received a bolus of 65 mg kg^{-1} alpha-Chloralose (α-Chloralose) solution in saline, administered through a tail vein cannula, followed by continuous infusion at a rate of 30 mg kg^{-1}h^{-1}.

All animals were scanned with the same protocol consisting of MP2-RAGE[26], ASL, and ASE images. The MP2-RAGE structural T1-weighted image was acquired with a matrix size of 160x160x128, isotropic 0.19mm voxel size, TE/TI1/TI2/TR = 2.7/900/3500/9000 ms, and flip-angles α_1/α_2 = 7/9°. An additional Ultrashort Echo Time (UTE) COMPOSER scan was acquired for coil combination[27].

For ASL we used the manufacturer's Continuous ASL (CASL) sequence with a spin-echo Echo Planar Imaging (EPI) readout[22]. The matrix size was 96x96 with 18 axial (rostro-caudal) slices, 0.26x0.26x1.5 mm voxel size, TE/TR = 13.5/4000 ms, partial-fourier 66%, label time 3000 ms, post-label time 300 ms[28,29], and 30 pairs of label/control images, scan time 4 minutes. The labelling plane was positioned 5 mm behind the carotid artery split, which was found using a localizer scan acquired with the labelling coil as per the manufacturer's instructions. Two single-volume reference scans were acquired using the same sequence settings and no labelling

power, one of which had reversed phase-encode direction (see below).

For the ASE sequence we modified the manufacturer's spin-echo EPI sequence to allow the 180° refocusing pulse to be offset by τ/2 as defined above. The matrix size and resolution were matched to the ASL sequence, but with TE/TR = 70/1800 ms. Partial Fourier was switched off to minimise any intensity modulation from the echo moving out of the acquisition window in the readout (X, left-right) direction[30]. Twelve values of τ spaced from -32 to 56 ms were acquired. At each, five Z-shims equally spaced from $G_Z = -0.8$ to $G_Z = 0.8$ mT m^{-1} and nine Y-shims from $G_Y = -1.2$ to $G_Y = 1.2$ mT m^{-1} were used. The Z-shim was incorporated into the slice-rephase gradient which lasted 2 ms and the Y-shim was played at the same time. The ASE scan lasted for 16 minutes and 12 seconds.

Image processing and analysis
Image processing was carried out using a combination of FSL 5.0.1[31], ANTs 2.1.0[32] and QUIT 3.3[33]. Briefly, the complex MP2-RAGE structural images were first coil-combined[27] and then converted into both a T1 map and a uniform contrast image[34]. From these, a study-specific template image was constructed[35] which was in turn registered to an atlas image[36]. Eleven bilateral Regions Of Interest (ROIs) were selected from the atlas and transformed to the template space: the Thalamus (Thl), Hypothalamus (HThl), Striatum (Stri), Inferior Colliculus (InfC), Cingulate Cortex (CgCx), Retrosplenial Cortex (RtCx), Insular Cortex (InCx), Corpus Callosum (CC), Septum (Sptm), Dorsal Hippocampus (DHip) and Peri-Aqueductal Grey Matter (PAG).

The CASL images were corrected for motion[37] and susceptibility distortions[38], and then converted into a CBF map using the BASIL tool[39]. The T1 of blood was set to 2.429 s[40], the labelling efficiency was set to 80%, and the distortion-corrected reference image was used as the proton density during CBF quantification[41]. The reference image was registered to the MP2-RAGE structural image.

The ASE images with different Z- & Y-shims were first combined by taking the Root Sum-of-Squares (RSS)[42]. To avoid noise amplification artefacts, we calculated the mean squared intensity in a background region and subtracted this from sum-of-squared images before taking the square root[43]. The resulting shimmed ASE images were then motion and distortion corrected using the ASL reference data. The OEF was found from the corrected data by a non-linear fit to Equation 2 implemented in QUIT[33]. We found that our images were too noisy to reliably fit for the parameter DBV, which is thought to be on the order of a few percent. To improve the quality of the fit for the remaining parameters we hence fixed DBV = 3.3%[23]. We also observed that in certain brain regions the peak of our signal curve did not occur precisely at τ = 0, hence we introduced an additional parameter ΔT to account for this. The final free parameters were R2′, S_0 & ΔT, from which the parameters T_c, dHb and most importantly OEF could be

derived. The resulting OEF and CBF maps were then multiplied together and by C_a to produce the $CMRO_2$ map. The parameter maps were resampled into the template space and average ROI values extracted using the template-specific masks.

Autoradiography protocol and analysis

To assess regional brain glucose metabolism we performed ^{14}C-2-deoxyglucose (2DG) autoradiography, which measures Glucose Utilisation (GU) in µmol/100g/min as originally described by Sokoloff[44]. We used a separate cohort of ten adult male Sprague Dawley rats (weight 325–380 g). All were initially anaesthetised for approximately 30 minutes with 2.5–3% isoflurane (in 80/20 medical air/oxygen), in order to cannulate their femoral and tail blood vessels for blood sampling and compound administration, respectively. After the cannulation, a local anaesthetic was applied and the wound sutured.

Isoflurane was then set to 2.5% for five rats. In the remaining rats, isoflurane was terminated and an intravenous bolus of 65 mg kg^{-1} α-Chloralose was administered, followed by 30 mg kg^{-1}h^{-1} infusion for the remainder of the experiment[45]. Body temperature was maintained at 36 ± 0.5°C using a thermostatically controlled electric heating blanket and rectal probe.

Between 30 and 40 minutes was allowed for the rats to stabilise, after which we intravenously administered over 30 s 100 µCi/kg 2DG (Perkin Elmer, USA), and collected 14 timed arterial blood samples[46] over 45 minutes. After the final blood sample the animals were decapitated. Their brains were removed and frozen in −40°C isopentane and then stored at −80°C. Quantification of plasma glucose and ^{14}C was carried out using a blood glucose analyser (YSI 2300) and scintillation counter (Beckman Coulter LS 6500), respectively. Brains were cryosectioned at 20 µm and exposed to X-ray film (Kodak Biomax MR-2) alongside calibrated ^{14}C standards (GE Healthcare UK) for 7 days, after which they were developed in an automated X-ray film processor. Images were digitised using a Nikon single lens reflex camera and a macro lens, over a Northern Lights illuminator (InterFocus Ltd UK). Brain GU was calculated from the optical densities in the films using a calibration curve and the plasma glucose levels according to 44. We measured GU in eleven ROIs which matched those chosen from the MRI atlas, located at approximately +1, -3.5 and -8 mm from Bregma[47]. Readings for each ROI were taken bilaterally from two or three adjacent brain sections and then averaged. The analyst was blinded to anaesthetic group.

Statistical analysis

For statistical analyses we used the Python libraries pandas 1.0.5 and statsmodels 0.11.1[48]. The mean ROI values for each anaesthetic were compared with a non-parametric Mann-Whitney U-test with False Discovery Rate (FDR) multiple-comparisons correction. Finally, we compared our MRI oxygen metabolism measurements to the glucose metabolism measurements using a Robust Linear Model analysis of $CMRO_2$ against GU. In this model, the slope of the line is the number of oxygen molecules consumed per molecule of

glucose during metabolic activity, while the intercept gives the amount of oxygen consumed if no glucose was being consumed. Robust regression was used because residual variance was inhomogenous across the metabolic range. As our experimental design did not use the same animals for both $CMRO_2$ and GU experiments, the measurements for each ROI were averaged across subjects (but not anaesthetics) before the regression, yielding a total of 22 data points for this analysis. For all analyses, a p-value of less than 0.05 was considered significant. ROI data and group average data are available in *Underlying data*[49].

Results

Pre-processing

Figure 1 and Figure 2 show a single slice through all the raw ASE images collected with different values of Z-&Y-shims at $\tau = 0$ and $\tau = 56$ ms, respectively. The central images have both G_Y and G_Z equal to zero, i.e. in Figure 1 this is a simple unshimmed symmetric spin-echo image. In Figure 1 only the central, low value shims contain significant signal and the extreme shims are mostly noise, whereas in Figure 2 the unshimmed image is mostly noise and the signal has shifted towards negative values of G_Y and G_Z.

Figure 3 shows the result of combining all the different shim images via RSS both with and without noise suppression. Without suppression, amplification of the Rician noise is so severe that the background has almost the same intensity as the image. Subtracting the mean squared background intensity before the square-root operation restores the correct noise properties to the image, with crisp contrast between the image and background regions.

Group comparisons

Figure 4 shows the results of the model fit to the shimmed ASE data. R2′ appears slightly higher in animals anaesthetised with α-Chloralose. Residual elevated R2′ can be observed surrounding the mastoid cavities and in a thin layer around the brain, where the Z-&Y-shimming was insufficient to correct extreme MFGs. The Root Mean Square Error (RMSE) is flat across most of the brain, indicating a reasonable model fit, but is elevated in white matter and cerebrospinal fluid (CSF), indicating the model fits less well in these areas. ΔT is increased towards the lower front of the brain.

Figure 5 shows the mean OEF, CBF and $CMRO_2$ for isoflurane and α-Chloralose anaesthetic. The OEF is higher under α-Chloralose. Areas with elevated R2′ due to MFGs also show artefactually high OEF. CBF is much lower under α-Chloralose anaesthetic than under isoflurane. The Inferior Colliculus shows an elevated CBF compared to other brain regions. $CMRO_2$ is consistently higher under isoflurane than under α-Chloralose.

In Figure 6 we display glucose consumption under both anaesthetics. Similarly to the MRI data, glucose metabolism is clearly reduced under α-Chloralose compared to isoflurane, and the Inferior Colliculus displays elevated metabolism compared to the rest of the brain.
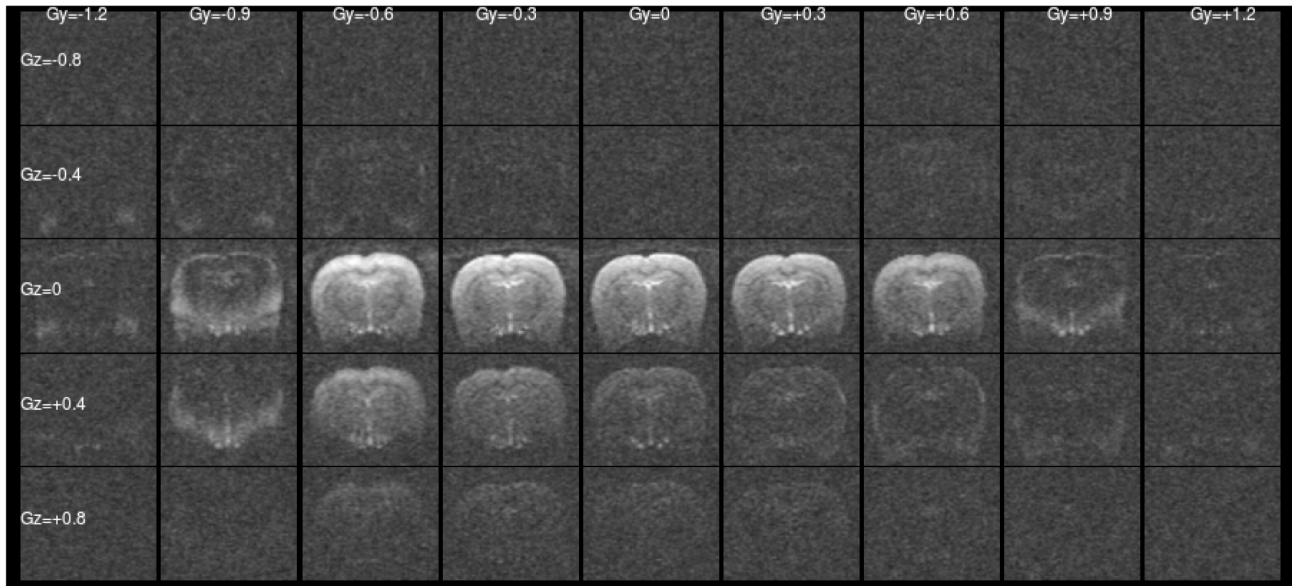
Figure 1. Raw asymmetric spin-echo data in a single slice at τ = 0 ms for all the values of Z- & Y-shims. The signal is concentrated at low shim values as expected.
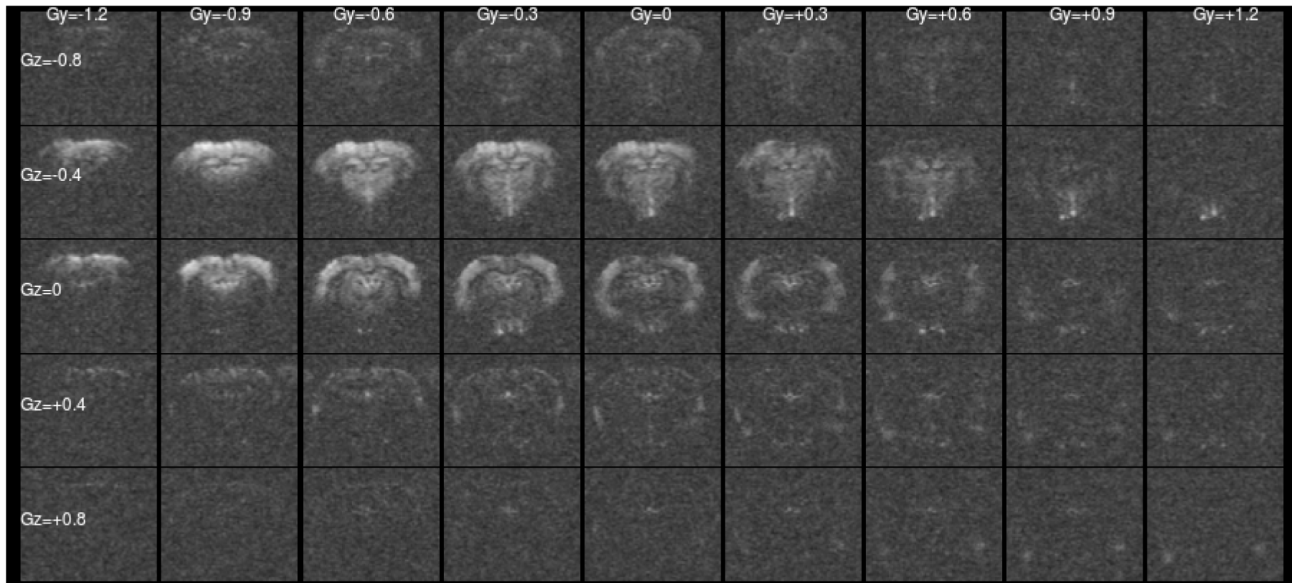
Figure 2. Asymmetric spin-echo data in a single slice at τ = 56 ms, as for Figure 1. For this highly asymmetric spin-echo, the signal energy has shifted towards more negative shim values, and the majority of the signal in the un-shimmed center image has been lost. Without shimming the signal would be erroneously low.

Table 1 gives the mean and standard deviation across subjects of each ROI for OEF, CBF, $CMRO_2$ and GU. Figure 7 shows the same data plotted graphically. $CMRO_2$, GU and CBF were all lower under α-Chloralose than isoflurane, while OEF was generally higher under α-Chloralose than isoflurane. These effects were strong and consistent for both CBF and Gu, with

perfect separation between α-Chloralose and isoflurane, i.e. all values in one group higher/lower than the other, with the exception of the Inferior Colliculus glucose consumption (Mann-Whitney U=22, FDR corrected p=0.17). For OEF there was some overlap between the groups, in particular the Hypothalamus showed equal OEF (U=12, FDR corrected p=1).
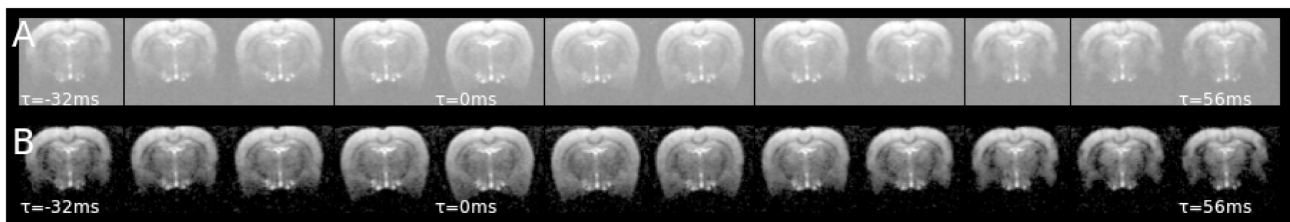
Figure 3. A The asymmetric spin-echo data after combining all shim values via naïve Root Sum-of-Squares. Noise has been amplified to the extent that the image cannot easily be distinguished from the background. **B** Noise suppression restores the signal-to-noise ratio to a reasonable level. The effect of R2′ decay can be observed at the high values of τ in cortical veins.
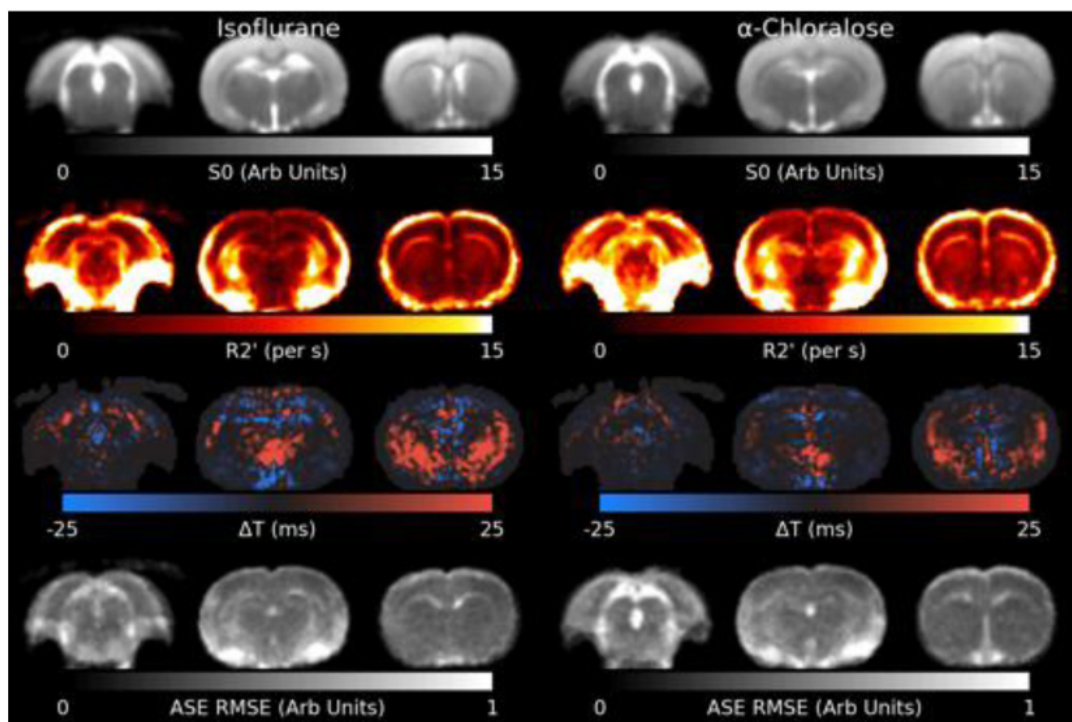
Figure 4. Slices through the fitted parameters and residual for the asymmetric spin-echo (ASE) data under both anaesthetics. R2′ values around the mastoid cavities are artifactually high. The model generally fits well across the brain, but is higher in white matter and cerebrospinal fluid. RMSE: Root Mean Square Error.

$CMRO_2$ hence showed a smaller separation than GU or CBF, which despite large non-parametric test statistics did not survive multiple comparisons correction (majority of ROIs U>=24, uncorrected p≤0.017, FDR corrected p=0.07).

Finally we show the result of regressing $CMRO_2$ against GU for the different regions of interest (averaged across subjects) in Figure 8. The slope of the line of best fit was 2.74 ($p < 0.001$, 95% CI 1.96 to 3.53).

Discussion

The above results demonstrate that $CMRO_2$ can be measured in rats using a combination of ASE and ASL images. The method does not require administration of a gas challenge[50,51], or administration of expensive isotopes[9]. Hence this method has the potential to be a cheap, easily available method compared to gold-standard PET measurements. Little *et al.* have demonstrated similar findings using separate measures of R2 and R2* to measure OEF instead of the single measurement of R2' from the ASE scan[52]. In humans, qBOLD has been combined with QSM to estimate $CMRO_2$ from a single multi-echo gradient-echo scan[12]. This method shows promise, but the required modelling and processing was extremely complex. In contrast, after correction for MFGs, the ASE method only requires a fit of Equation (2) to the data. We then combined our measurement of OEF with CBF measured by ASL to generate a map of
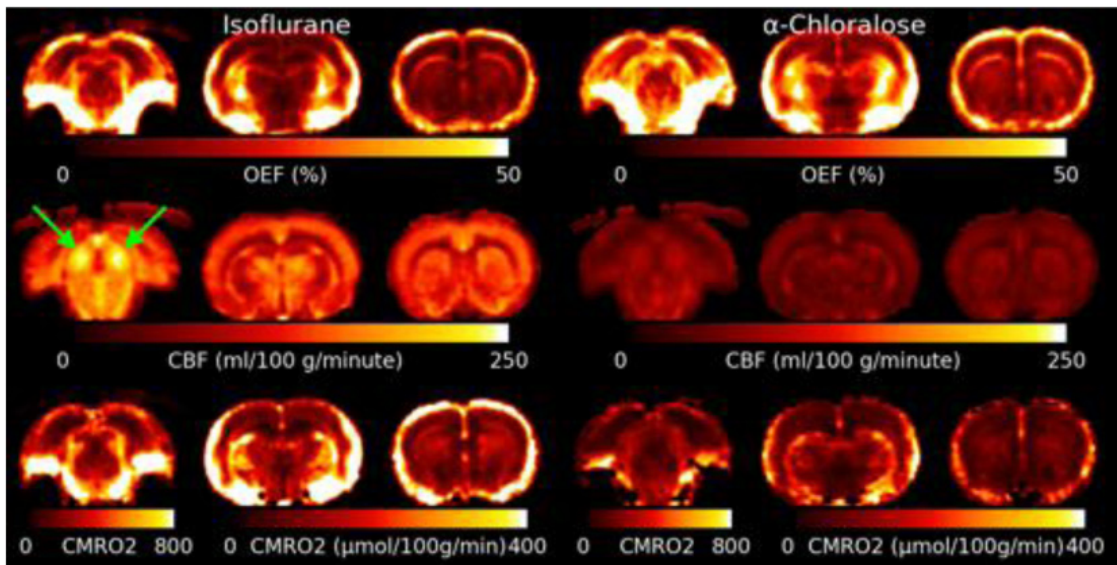
Figure 5. Slices through the mean Oxygen Extraction Fraction (OEF), Cerebral Blood Flow (CBF) and Cerebral Metabolic Rate of Oxygen (CMRO$_2$) for both anaesthetics. CMRO$_2$ is lower under α-Chloralose, however this is driven by a significant reduction in CBF as OEF is actually higher under α-Chloralose than isoflurane. Note that the slice through the inferior colliculus (marked with green arrows) for CMRO$_2$ has a different color scale due to the much higher rate of metabolism compared to the other slices.
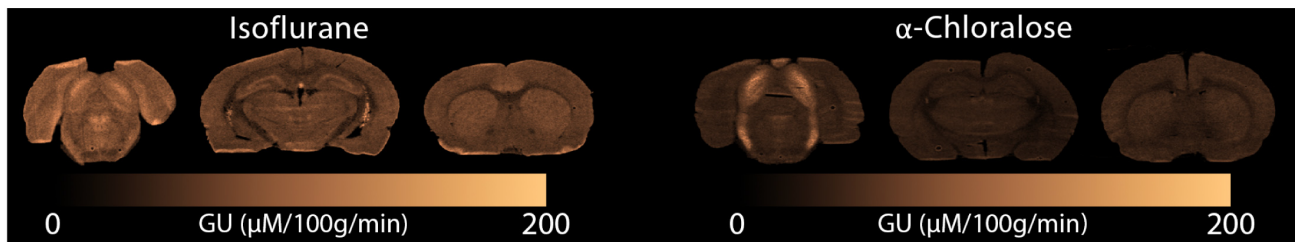
Figure 6. Glucose consumption measured with autoradiography under (left) isoflurane and (right) α-Chloralose. GU: Glucose Utilisation.

CMRO$_2$ under two common anaesthetics which are known to have different effects on brain metabolism. By using a dedicated labelling coil and correcting our multi-slice 2D data with the correct post-label delay we obtained full brain maps of CBF[39,53].

There were numerous technical challenges to implementing the ASE method at ultra-high field (9.4T) and the small dimensions of a preclinical system compared to previous clinical work. Foremost, MFGs were highly problematic, and adequately correcting them involved a large number of trade-offs which prevented full correction across all regions of the brain. Notably, we observed strong gradients in all three geometric directions. This required the implementation of shimming in both the slice-select (Z) and phase-encode (Y) directions. Providing an adequate number of shims required acquiring a total of 45 images per value of τ (nine Y-shims multiplied by 5 Z-shims), which is significantly more than the eight images

that were adequate in a clinical setting[19]. Including shim gradients in the readout direction (X) may have further reduced MFG artefacts, but at the expense of additional scan-time.

Thinner slices would also reduce the impact of the MFGs, but would also lower signal-to-noise ratio (SNR) and brain coverage. Acquiring more slices would be problematic for the ASL scan, where the maximum number is determined by the time between the end of the post-labelling time and the end of TR. Increasing TR and hence the number of slices would hence increase the ASL scan time further and lead to very different post-labelling times for different slices.

As shown in Figure 2, naïve RSS combination of the different shims leads to amplification of the Rician noise in low signal areas. We could not use the Fourier Transform approach to shim combination taken by Stone & Blockley[19] as the

Table 1. Mean and standard deviation of each parameter value in each Regions of Interest (ROI), and the average across the ROIs. OEF, Oxygen Extraction Fraction; CMRO2, Cerebral Metabolic Rate of Oxygen; CBF, Cerebral Blood Flow; GU, Glucose Utilisation.

| ROI	OEF (%)		CBF (ml/100g/min)		CMRO$_2$ (µmol/100g/min)		GU (µmol/100g/min)	
	Iso	αCl	Iso	αCl	Iso	αCl	Iso	αCl
Stri	14.9±1.1	18.9±1.1	134.8±29.8	61.3±29.8	155.1±40.6	92.7±40.6	93.5±19.3	52.9±19.3
CnCx	11.2±1.9	18.0±1.9	136.2±22.6	44.5±22.6	120.7±5.8	68.9±5.8	88.3±19.7	48.1±19.7
CC	17.3±1.2	21.9±1.2	92.6±17.2	39.7±17.2	125.4±26.2	63.2±26.2	55.4±10.3	35.1±10.3
RtCx	10.3±2.1	18.2±2.1	144.0±20.5	58.6±20.5	132.6±23.2	103.2±23.2	77.6±14.4	45.1±14.4
Thl	16.9±2.8	22.9±2.8	146.1±43.6	51.5±43.6	177.9±39.8	89.4±39.8	86.9±11.1	50.9±11.1
InCl	26.5±2.9	34.5±2.9	201.4±48.4	78.4±48.4	421.5±69.0	216.4±69.0	119.0±25.3	80.5±25.3
InCx	22.4±4.5	26.5±4.5	138.1±25.2	52.6±25.2	271.1±38.6	122.5±38.6	86.6±19.8	53.7±19.8
Sptm	10.8±1.8	14.9±1.8	122.5±30.1	47.1±30.1	109.6±36.5	61.8±36.5	73.6±18.4	42.1±18.4
HThl	18.2±2.6	18.1±2.6	139.9±35.2	54.5±35.2	222.6±76.7	80.9±76.7	76.9±17.1	44.6±17.1
DHip	12.3±2.1	22.0±2.1	125.0±25.1	49.9±25.1	141.1±28.1	103.3±28.1	77.7±13.3	47.3±13.3
PAG	14.2±1.3	19.1±1.3	164.8±42.9	62.7±42.9	186.2±46.9	94.6±46.9	78.2±16.2	48.2±16.2
Avg	15.9±5.3	21.3±5.3	140.5±38.8	54.6±38.8	187.6±95.6	99.7±95.6	83.1±21.5	49.9±21.5
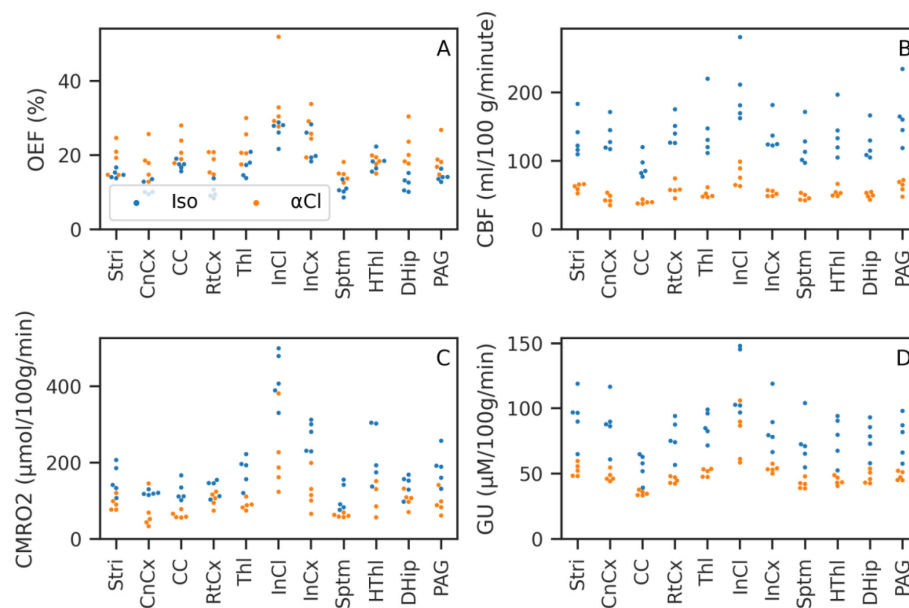
Figure 7. Mean value of Oxygen Extraction Fraction (OEF), Cerebral Blood Flow (CBF), Cerebral Metabolic Rate of Oxygen (CMRO$_2$), and Glucose Utilisation (GU) in the chosen Regions of Interest (ROIs) for each subject. CMRO$_2$ and GU consumption are both reduced under α-Chloralose anaesthetic compared to isoflurane. Almost total separation between the two groups was achieved; ROIs and parameters where this did not occur are noted in the text.

necessary reconstruction methods were not available from the manufacturer. Subtracting the average noise level from the squared magnitude images restored an adequate level of SNR. It is possible that using a method that accounts for the multi-channel nature of this data could improve the SNR further[54,55].
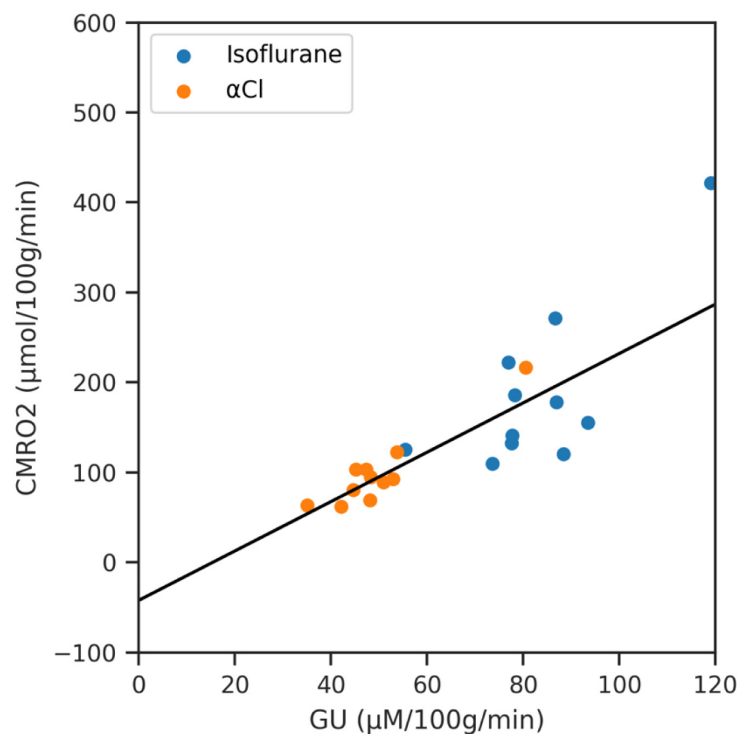
Figure 8. A regression analysis of Cerebral Metabolic Rate of Oxygen (CMRO$_2$) against Glucose Utilisation (GU) across the averaged regions of interest data for both anaesthetics.

Despite this, we found we could not reliably fit for both DBV and R2' (data not shown). Little *et al.* used a separate Turbo Dynamic ASL scan to measure arterial blood volume, and then assumed a fixed venous/arterial blood volume ratio[52]. As we did not acquire such a scan, we fixed DBV to a single value. Previous literature values of DBV in healthy humans vary from 1%[56] to 3.6%[18]. In rodents Yablonskiy *et al.* reported a value of 3.3%, Little *et al.* reported 3.15%[23,52], and Sandor *et al.* reported 3.5% (after conversion from CBV)[57]. We opted to use the former value. Fixing DBV in this manner is not ideal as it will vary due to pathology[52]. We hypothesise that adjusting the protocol to acquire fewer intermediate values of τ and additional images with high values and near $\tau=0$ could improve the sensitivity to both DBV and R2'[58]. Increasing the maximum value of τ would necessitate either a corresponding increase in TE, which would reduce SNR and increase the effects of MFGs[19], or the use of Partial Fourier acceleration, which we found caused unacceptable blurring and intensity artefacts from the echo moving out of the EPI acquisition window[30]. Using an alternate readout such as spiral imaging may mitigate such downsides. Such optimization was beyond the scope of the current work.

The introduction of the parameter ΔT, representing either the early or late arrival of the spin-echo peak, improved the stability of our fit on the edges of white matter and towards the lower front portion of the brain. We hypothesise that that these shifts were due to uncorrected MFGs, either in the X-direction causing signal to shift away from the k-space center at $\tau=0$[30,59], or simply insufficient correction in the Y- and Z-directions. Further investigation of this was beyond the scope of the current work. We showed both an increase in OEF and root-mean-square error in white-matter regions, indicating that the current model does not account properly for the effects of myelin, which has a different susceptibility to other brain tissue[60].

Comparing our measured values of CBF, OEF and CMRO$_2$ to existing literature is complicated by a wide range of measurement techniques, regions of interest, anesthetic regimes, and potential inter-species differences with humans. Starting with CBF, where the pre-clinical literature is better developed, our results appear in line with existing work. Masamoto and Kanno summarized previous literature on CBF measured by MRI and autoradiography and reported values between 102 and 247 ml/100g/min depending on the level of isoflurane anesthesia, and only 65 ml/100g/min for α-Chloralose measured by autoradiography[61]. Little *et al.* reported 99–115 ml/100g/min under 1.5–2% isoflurane[52], while Lenz *et al.* reported 124–150 ml/100g/min depending on the level of isoflurane[62]. We hence conclude that our CBF measurement broadly agrees with previous literature.

Previous estimates of OEF in healthy humans are 35%, measured with calibrated gas administration[13], and 21% using the same ASE method used here[19], however we note that the authors acknowledged that their choice of linear fitting deliberately underestimates OEF. Hyder *et al.* found an average grey matter OEF of 40% using PET imaging[63]. In rats, Little *et al.* found values between 35 and 40% under Isoflurane anesthesia using an R2' method similar to ours[52]. He *et al.* reported mean OEFs of 23% and 38% under isoflurane and α-Chloralose respectively[23]. This comparison to previous literature would indicate that the method presented here underestimates OEF.

Previous reported measures of $CMRO_2$ in rats under α-chloralose anesthetic range include 151[7], 184[64], 200[65], 208[66] and 219[67] μmol/100g/min. Our reported $CMRO_2$ is approximately half that of the most commonly reported, and almost certainly due to the underestimate of OEF identified above.

Further evidence for this underestimation comes from the work of Hyder *et al.*, who measured $CMRO_2$ and GU in awake humans using PET and found an Oxygen Glucose Index (OGI) of 5.3. Under pure aerobic metabolism, the stoichiometric ratio of six molecules of oxygen to one molecule of glucose would suggest an OGI of six[68,69]. The average OGI is equivalent to the slope of our $CMRO_2$ / GU regression line, which we found to be only 2.74. Although inter-species and anesthetic effects cannot be discounted, we attribute this discrepancy to our underestimation of OEF. As discussed above, a likely cause of this underestimation is the choice of equally spread τ values, and an optimized protocol may lead to more accurate OEF estimation.

It is also possible that some of the constants chosen here may be incorrect. An obvious candidate would be the chosen value of DBV, as this roughly scales the estimate of OEF. However, decreasing the value of DBV such that our $CMRO_2$ estimates agreed with literature values would require approximately halving it, which would then make the estimate of DBV itself significantly different to previous literature.

Despite this underestimation, we confirmed the expected differential effect of the anesthetics on cerebral metabolism, with close to double the rate of oxygen consumption under isoflurane than α-Chloralose. We note that the difference in $CMRO_2$ was driven primarily by the difference in CBF which was three times higher under isoflurane, while OEF only reduced by a quarter compared to α-Chloralose. This is in line with the notion that mitochondria require a particular gradient of tissue oxygenation, and because less oxygen is removed from the blood during higher flow (decreased capillary transit time), it follows that OEF is decreased with increased CBF and $CMRO_2$[70].

Conclusions

We implemented a non-invasive MRI method for measuring $CMRO_2$ in rats which can be easily translated to clinical scanners. Methodological difficulties prevented measurement of DBV and we likely underestimated OEF, but future optimizations may be able to overcome these limitations. However the relative $CMRO_2$ differences between anesthetics were observed, suggesting the utility of this relatively simple method for preclinical studies interested in comparing metabolic effects of treatments or pathologies.

Data availability

Underlying data

Figshare: $CMRO_2$ in Rodents. https://doi.org/10.6084/m9.figshare.14199035.v3[49].

This project contains the following underlying data:

-ROIS (ROI summary statistics in Comma Separated Value format).

-Parameter maps (mean parameter maps in Nifti format).

-Raw ASE scans (in Nifti format).

Data are available under the terms of the Creative Commons Attribution 4.0 International license (CC-BY 4.0).

References

1. Hofman MA: **Energy metabolism, brain size and longevity in mammals.** *Q Rev Biol.* 1983; **58**(4): 495–512.
   PubMed Abstract | **Publisher Full Text**

2. Clarke DD, Sokoloff L: **Regulation of cerebral metabolic rate.** *Basic neurochemistry: molecular, cellular and medical aspects.* 1999; 6.
   Reference Source

3. Ishii K, Kitagaki H, Kono M, *et al.*: **Decreased medial temporal oxygen metabolism in Alzheimer's disease shown by PET.** *J Nucl Med.* 1996; **37**(7): 1159–65.
   PubMed Abstract

4. Lee JM, Vo KD, An H, *et al.*: **Magnetic resonance cerebral metabolic rate of oxygen utilization in hyperacute stroke patients.** *Ann Neurol.* 2003; **53**(2): 227–232.
   PubMed Abstract | **Publisher Full Text**

5. Ge Y, Zhang Z, Lu H, *et al.*: **Characterizing brain oxygen metabolism in patients with multiple sclerosis with *T2*-relaxation-under-spin-tagging MRI.** *J Cereb Blood Flow Metab.* 2012; **32**(3): 403–412.
   PubMed Abstract | **Publisher Full Text** | **Free Full Text**

6. Catchlove SJ, Macpherson H, Hughes ME, *et al.*: **An investigation of cerebral oxygen utilization, blood flow and cognition in healthy aging.** *PLoS One.* 2018; **13**(5): e0197055.
   PubMed Abstract | **Publisher Full Text** | **Free Full Text**

7. Zhu XH, Zhang Y, Zhang N, *et al.*: **Noninvasive and Three-Dimensional Imaging of CMRO(2) in Rats at 9.4 T: Reproducibility Test and Normothermia/Hypothermia Comparison Study.** *J Cereb Blood Flow Metab.* 2007; **27**(6): 1225–1234.
   PubMed Abstract | **Publisher Full Text**

8. Watabe T, Shimosegawa E, Watabe H, *et al.*: **Quantitative Evaluation of Cerebral Blood Flow and Oxygen Metabolism in Normal Anesthetized Rats: ¹⁵O-Labeled Gas Inhalation PET with MRI Fusion.** *J Nucl Med.* 2013; **54**(2): 283–290.
   PubMed Abstract | **Publisher Full Text**

9. Kurzhunov D, Borowiak R, Hass H, *et al.*: **Quantification of oxygen metabolic rates in Human brain with dynamic ¹⁷ O MRI: Profile likelihood analysis.** *Magn Reson Med.* 2017; **78**(3): 1157–1167.
   PubMed Abstract | **Publisher Full Text**

10. Liu P, Huang H, Rollins N, *et al.*: **Quantitative assessment of global cerebral metabolic rate of oxygen (CMRO₂) in neonates using MRI.** *NMR Biomed.* 2014; **27**(3): 332–340.
PubMed Abstract | **Publisher Full Text** | **Free Full Text**

11. Wehrli FW, Fan AP, Rodgers ZB, *et al.*: **Susceptibility-based time-resolved whole-organ and regional tissue oximetry.** *NMR Biomed.* 2017; **30**(4): e3495.
PubMed Abstract | **Publisher Full Text** | **Free Full Text**

12. Cho J, Kee Y, Spincemaille P, *et al.*: **Cerebral metabolic rate of oxygen (CMRO₂) mapping by combining quantitative susceptibility mapping (QSM) and quantitative blood oxygenation level-dependent imaging (qBOLD).** *Magn Reson Med.* 2018; **80**(4): 1595–1604.
PubMed Abstract | **Publisher Full Text** | **Free Full Text**

13. Bulte DP, Kelly M, Germuska M, *et al.*: **Quantitative measurement of cerebral physiology using respiratory-calibrated MRI.** *Neuroimage.* 2012; **60**(1): 582–591.
PubMed Abstract | **Publisher Full Text** | **Free Full Text**

14. Blockley NP, Griffeth VE, Stone AJ, *et al.*: **Sources of systematic error in calibrated BOLD based mapping of baseline oxygen extraction fraction.** *Neuroimage.* 2015; **122**: 105–113.
PubMed Abstract | **Publisher Full Text**

15. Zhang J, Liu T, Gupta A, *et al.*: **Quantitative mapping of cerebral metabolic rate of oxygen (CMRO₂) using quantitative susceptibility mapping (QSM).** *Magn Reson Med.* 2015; **74**(4): 945–52.
PubMed Abstract | **Publisher Full Text** | **Free Full Text**

16. Alsop DC, Detre JA, Golay X, *et al.*: **Recommended implementation of arterial spin-labeled perfusion MRI for clinical applications: A consensus of the ISMRM perfusion study group and the European consortium for ASL in dementia.** *Magn Reson Med.* 2015; **73**(1): 102–116.
PubMed Abstract | **Publisher Full Text** | **Free Full Text**

17. Yablonskiy DA, Haacke EM: **Theory of NMR signal behavior in magnetically inhomogeneous tissues: The static dephasing regime.** *Magn Reson Med.* 1994; **32**(6): 749–763.
PubMed Abstract | **Publisher Full Text**

18. Blockley NP, Stone AJ: **Improving the specificity of R₂′ to the deoxyhaemoglobin content of brain tissue: Prospective correction of macroscopic magnetic field gradients.** *Neuroimage.* 2016; **135**: 253–260.
PubMed Abstract | **Publisher Full Text**

19. Stone AJ, Blockley NP: **A streamlined acquisition for mapping baseline brain oxygenation using quantitative BOLD.** *Neuroimage.* 2017; **147**: 79–88.
PubMed Abstract | **Publisher Full Text**

20. Gagnon L, Sakadžić S, Lesage F, *et al.*: **Quantifying the Microvascular Origin of BOLD-fMRI from First Principles with Two-Photon Microscopy and an Oxygen-Sensitive Nanoprobe.** *J Neurosci.* 2015; **35**(8): 3663–3675.
PubMed Abstract | **Publisher Full Text** | **Free Full Text**

21. Václavů L, Petr J, Petersen ET, *et al.*: **Cerebral oxygen metabolism in adults with sickle cell disease.** *Am J Hematol.* 2020; **95**(4): 401–412.
PubMed Abstract | **Publisher Full Text** | **Free Full Text**

22. Wong EC: **An introduction to ASL labeling techniques.** *J Magn Reson Imaging.* 2014; **40**(1): 1–10.
PubMed Abstract | **Publisher Full Text**

23. He X, Zhu M, Yablonskiy DA: **Validation of oxygen extraction fraction measurement by qBOLD technique.** *Magn Reson Med.* 2008; **60**(4): 882–888.
PubMed Abstract | **Publisher Full Text** | **Free Full Text**

24. Frahm J, Merboldt KD, Hänicke W: **Direct FLASH MR imaging of magnetic field inhomogeneities by gradient compensation.** *Magn Reson Med.* 1988; **6**(4): 474–480.
PubMed Abstract | **Publisher Full Text**

25. Ordidge RJ, Gorell JM, Deniau JC, *et al.*: **Assessment of relative brain iron concentrations using T_2-weighted and T_2*-weighted MRI at 3 Tesla.** *Magn Reson Med.* 1994; **32**(3): 335–341.
PubMed Abstract | **Publisher Full Text**

26. Marques JP, Kober T, Krueger G, *et al.*: **MP2RAGE, a self bias-field corrected sequence for improved segmentation and T_1-mapping at high field.** *Neuroimage.* 2010; **49**(2): 1271–1281.
PubMed Abstract | **Publisher Full Text**

27. Robinson SD, Dymerska B, Bogner W, *et al.*: **Combining phase images from array coils using a short echo time reference scan (COMPOSER).** *Magn Reson Med.* 2017; **77**(1): 318–327.
PubMed Abstract | **Publisher Full Text** | **Free Full Text**

28. Thomas DL, Lythgoe MF, van der Weerd L, *et al.*: **Regional Variation of Cerebral Blood Flow and Arterial Transit Time in the Normal and Hypoperfused Rat Brain Measured Using Continuous Arterial Spin Labeling MRI.** *J Cereb Blood Flow Metab.* 2006; **26**(2): 274–282.
PubMed Abstract | **Publisher Full Text**

29. Wells JA, Lythgoe MF, Choy M, *et al.*: **Characterizing the Origin of the Arterial Spin Labelling Signal in MRI Using a Multiecho Acquisition Approach.** *J Cereb Blood Flow Metab.* 2009; **29**(11): 1836–1845.
PubMed Abstract | **Publisher Full Text**

30. Weiskopf N, Hutton C, Josephs O, *et al.*: **Optimized EPI for fMRI studies of the orbitofrontal cortex: compensation of susceptibility-induced gradients in the readout direction.** *MAGMA.* 2007; **20**(1): 39–49.
PubMed Abstract | **Publisher Full Text** | **Free Full Text**

31. Jenkinson M, Beckmann CF, Behrens TE, *et al.*: **FSL.** *Neuroimage.* 2012; **62**(2): 782–790.
PubMed Abstract | **Publisher Full Text**

32. Avants BB, Tustison NJ, Song G, *et al.*: **A reproducible evaluation of ANTs similarity metric performance in brain image registration.** *Neuroimage.* 2011; **54**(3): 2033–2044.
PubMed Abstract | **Publisher Full Text** | **Free Full Text**

33. Wood TC: **QUIT: QUantitative Imaging Tools.** *J Open Res Softw.* 2018; **3**(26): 656.
Publisher Full Text

34. O'Brien KR, Kober T, Hagmann P, *et al.*: **Robust T1-Weighted Structural Brain Imaging and Morphometry at 7T Using MP2RAGE.** *PLoS One.* 2014; **9**(6): e99676.
PubMed Abstract | **Publisher Full Text** | **Free Full Text**

35. Avants BB, Yushkevich P, Pluta J, *et al.*: **The optimal template effect in hippocampus studies of diseased populations.** *Neuroimage.* 2010; **49**(3): 2457–2466.
PubMed Abstract | **Publisher Full Text** | **Free Full Text**

36. Valdés-Hernández PA, Sumiyoshi A, Nonaka H, *et al.*: **An *in vivo* MRI template set for morphometry, tissue segmentation, and fMRI localization in rats.** *Front Neuroinform.* 2011; **5**: 26.
PubMed Abstract | **Publisher Full Text** | **Free Full Text**

37. Jenkinson M, Bannister P, Brady M, *et al.*: **Improved Optimization for the Robust and Accurate Linear Registration and Motion Correction of Brain Images.** *Neuroimage.* 2002; **17**(2): 825–841.
PubMed Abstract | **Publisher Full Text**

38. Andersson JLR, Skare S, Ashburner J: **How to correct susceptibility distortions in spin-echo echo-planar images: application to diffusion tensor imaging.** *Neuroimage.* 2003; **20**(2): 870–888.
PubMed Abstract | **Publisher Full Text**

39. Chappell MA, Groves AR, Whitcher B, *et al.*: **Variational Bayesian Inference for a Nonlinear Forward Model.** *IEEE Trans Signal Process.* 2009; **57**(1): 223–236.
Publisher Full Text

40. Dobre MC, Uğurbil K, Marjanska M: **Determination of blood longitudinal relaxation time (T1) at high magnetic field strengths.** *Magn Reson Imaging.* 2007; **25**(5): 733–735.
PubMed Abstract | **Publisher Full Text**

41. Pinto J, Chappell MA, Okell TW, *et al.*: **Calibration of arterial spin labeling data-potential pitfalls in post-processing.** *Magn Reson Med.* 2020; **83**(4): 1222–1234.
PubMed Abstract | **Publisher Full Text** | **Free Full Text**

42. Constable RT, Spencer DD: **Composite image formation in z-shimmed functional MR imaging.** *Magn Reson Med.* 1999; **42**(1): 110–117.
PubMed Abstract | **Publisher Full Text**

43. Miller AJ, Joseph PM: **The use of power images to perform quantitative analysis on low SNR MR images.** *Magn Reson Imaging.* 1993; **11**(7): 1051–1056.
PubMed Abstract | **Publisher Full Text**

44. Sokoloff L, Reivich M, Kennedy C, *et al.*: **The [¹⁴C]deoxyglucose method for the measurement of local cerebral glucose utilization: theory, procedure, and normal values in the conscious and anesthetized albino rat.** *J Neurochem.* 1977; **28**(5): 897–916.
PubMed Abstract | **Publisher Full Text**

45. Duricki DA, Hutson TH, Kathe C, *et al.*: **Delayed intramuscular human neurotrophin-3 improves recovery in adult and elderly rats after stroke.** *Brain.* Publisher: Oxford University Press, 2016; **139**(Pt 1): 259–275.
PubMed Abstract | **Publisher Full Text** | **Free Full Text**

46. Littlewood CL, Cash D, Dixon AL, *et al.*: **Using the BOLD MR signal to differentiate the stereoisomers of ketamine in the rat.** *Neuroimage.* 2006; **32**(4): 1733–1746.
PubMed Abstract | **Publisher Full Text**

47. Paxinos G, Watson C: **The rat brain in stereotaxic coordinates: hard cover edition**. Elsevier, 2006.
Reference Source

48. Seabold S, Perktold J: **statsmodels: Econometric and statistical modeling with python.** In: *9th python in science conference.* 2010.
Reference Source

49. Wood T: **CMRO2 in Rodents.** figshare. Dataset. 2021.
http://www.doi.org/10.6084/m9.figshare.14199035.v3

50. Blockley NP, Griffeth VE, Simon AB, *et al.*: **A review of calibrated blood oxygenation level-dependent (BOLD) methods for the measurement of task-induced changes in brain oxygen metabolism.** *NMR Biomed.* 2013; **26**(8): 987–1003.
PubMed Abstract | **Publisher Full Text** | **Free Full Text**

51. Peng SL, Ravi H, Sheng M, *et al.*: **Searching for a truly "iso-metabolic" gas challenge in physiological MRI.** *J Cereb Blood Flow Metab.* 2017; **37**(2): 715–725.
PubMed Abstract | **Publisher Full Text** | **Free Full Text**

52. Little PV, Kraft SE, Chireh A, *et al.*: **Oxygen metabolism MRI – A comparison with perfusion imaging in a rat model of MCA branch occlusion and reperfusion.** *J Cereb Blood Flow Metab.* 2020; **40**(11): 2315–2327.
PubMed Abstract | **Publisher Full Text** | **Free Full Text**

53. Zaharchuk G, Ledden PJ, Kwong KK, *et al.*: **Multislice perfusion and perfusion**

territory imaging in humans with separate label and image coils. *Magn Reson Med.* 1999; **41**(6): 1093–1098.
PubMed Abstract | **Publisher Full Text**

54. Koay CG, Basser PJ: **Analytically exact correction scheme for signal extraction from noisy magnitude MR signals.** *J Magn Reson.* 2006; **179**(2): 317–322.
PubMed Abstract | **Publisher Full Text**

55. Bai R, Koay CG, Hutchinson E, *et al.*: **A framework for accurate determination of the T_2 distribution from multiple echo magnitude MRI images.** *J Magn Reson.* 2014; **244**: 53–63.
PubMed Abstract | **Publisher Full Text** | **Free Full Text**

56. He X, Yablonskiy DA: **Quantitative BOLD: Mapping of human cerebral deoxygenated blood volume and oxygen extraction fraction: Default state.** *Magn Reson Med.* 2007; **57**(1): 115–126.
PubMed Abstract | **Publisher Full Text** | **Free Full Text**

57. Sandor P, Cox-van Put J, de Jong W, *et al.*: **Continuous measurement of cerebral blood volume in rats with the photoelectric technique: Effect of morphine and naloxone.** *Life Sci.* 1986; **39**(18): 1657–1665.
PubMed Abstract | **Publisher Full Text**

58. Cercignani M, Alexander DC: **Optimal acquisition schemes for in vivo quantitative magnetization transfer MRI.** *Magn Reson Med.* 2006; **56**(4): 803–810.
PubMed Abstract | **Publisher Full Text**

59. Chen NK, Oshio K, Panych LP: **Application of k-space energy spectrum analysis to susceptibility field mapping and distortion correction in gradient-echo EPI.** *Neuroimage.* 2006; **31**(2): 609–622.
PubMed Abstract | **Publisher Full Text**

60. Schweser F, Sommer K, Deistung A, *et al.*: **Quantitative susceptibility mapping for investigating subtle susceptibility variations in the human brain.** *Neuroimage.* 2012; **62**(3): 2083–2100.
PubMed Abstract | **Publisher Full Text**

61. Masamoto K, Kanno I: **Anesthesia and the Quantitative Evaluation of Neurovascular Coupling.** *J Cereb Blood Flow Metab.* 2012; **32**(7): 1233–1247.
PubMed Abstract | **Publisher Full Text** | **Free Full Text**

62. Lenz C, Rebel A, van Ackern K, *et al.*: **Local Cerebral Blood Flow, Local Cerebral Glucose Utilization, and Flow-Metabolism Coupling during Sevoflurane versus Isoflurane Anesthesia in Rats.** *Anesthesiology.* 1998; **89**(6): 1480–1488.
PubMed Abstract | **Publisher Full Text**

63. Hyder F, Herman P, Bailey CJ, *et al.*: **Uniform distributions of glucose oxidation and oxygen extraction in gray matter of normal human brain: No evidence of regional differences of aerobic glycolysis.** *J Cereb Blood Flow Metab.* 2016; **36**(5): 903–916.
PubMed Abstract | **Publisher Full Text** | **Free Full Text**

64. Hyder F, Kennan RP, Kida I, *et al.*: **Dependence of Oxygen Delivery on Blood Flow in Rat Brain: A 7 Tesla Nuclear Magnetic Resonance Study.** *J Cereb Blood Flow Metab.* 2000; **20**(3): 485–498.
PubMed Abstract | **Publisher Full Text**

65. Zhang N, Zhu XH, Lei H, *et al.*: **Simplified Methods for Calculating Cerebral Metabolic Rate of Oxygen Based on ^{17}O Magnetic Resonance Spectroscopic Imaging Measurement during a Short $^{17}O_2$ Inhalation.** *J Cereb Blood Flow Metab.* 2004; **24**(8): 840–848.
PubMed Abstract | **Publisher Full Text**

66. Yee SH, Lee K, Jerabek PA, *et al.*: **Quantitative measurement of oxygen metabolic rate in the rat brain using microPET imaging of briefly inhaled ^{15}O-labelled oxygen gas.** *Nucl Med Commun.* 2006; **27**(7): 573–581.
PubMed Abstract | **Publisher Full Text**

67. Zhu XH, Zhang Y, Tian RX, *et al.*: **Development of (^{17}O) NMR approach for fast imaging of cerebral metabolic rate of oxygen in rat brain at high field.** *Proc Natl Acad Sci U S A.* 2002; **99**(20): 13194–13199.
PubMed Abstract | **Publisher Full Text** | **Free Full Text**

68. Mergenthaler P, Lindauer U, Dienel GA, *et al.*: **Sugar for the brain: the role of glucose in physiological and pathological brain function.** *Trends Neurosci.* 2013; **36**(10): 587–597.
PubMed Abstract | **Publisher Full Text** | **Free Full Text**

69. Goyal MS, Hawrylycz M, Miller JA, *et al.*: **Aerobic Glycolysis in the Human Brain Is Associated with Development and Neotenous Gene Expression.** *Cell Metab.* 2014; **19**(1): 49–57.
PubMed Abstract | **Publisher Full Text** | **Free Full Text**

70. Buxton RB: **Coupling between CBF and $CMRO_2$ during neuronal activity.** *Int Congr Ser.* 2002; **1235**: 23–32.
Publisher Full Text

Open Peer Review

Current Peer Review Status: ✓ ✓

Version 4

Reviewer Report 30 August 2022

https://doi.org/10.21956/wellcomeopenres.20159.r52156

✓
Avery Berman (iD)

[1] Athinoula A. Martinos Center for Biomedical Imaging, Massachusetts General Hospital, Charlestown, MA, USA
[2] Department of Physics, Carleton University, Ottawa, ON, Canada
[3] Brain Imaging Centre, The Royal Ottawa Institute of Mental Health Research, Ottawa, ON, Canada

The authors have shown that they have thoroughly examined the issue of the shift of the R2' decay curve. My comments have been addressed.

Competing Interests: No competing interests were disclosed.

Reviewer Expertise: biophysical modelling of the blood oxygenation level-dependent (BOLD) fMRI signal, high-resolution fMRI, MRI pulse sequence development

I confirm that I have read this submission and believe that I have an appropriate level of expertise to confirm that it is of an acceptable scientific standard.

Version 3

Reviewer Report 27 July 2022

https://doi.org/10.21956/wellcomeopenres.20005.r51500

?

Avery Berman [iD]

[1] Athinoula A. Martinos Center for Biomedical Imaging, Massachusetts General Hospital, Charlestown, MA, USA

[2] Department of Physics, Carleton University, Ottawa, ON, Canada

[3] Brain Imaging Centre, The Royal Ottawa Institute of Mental Health Research, Ottawa, ON, Canada

1. Perhaps examining the multi-channel combination on top of the shim combination is beyond the scope of the study. This could be examined in more detail in another study and the addition to the Discussion in the revised submission is appropriate.

2. Regarding the shift parameter, ΔT, its presence was surprising since it would seem to imply that the signal when $\tau \neq 0$ can be greater than the signal at $\tau = 0$ (i.e., the spin-echo itself). I did not originally list any ways that the authors could try to investigate the origins of the shift because I did not want to impose one way when the authors may have preferred some other, which too could have been appropriate. Some combination of the techniques that I had in mind were (I am not asking that you perform all these suggested analyses!):

   a) Probably the most direct test would be to simulate/calculate the asymmetric spin-echo sequence (ignoring image encoding) with a range of τ offsets in a voxel with or without a static field inhomogeneity across it. Next, add various magnitudes of blipped shims. How does the "decay" curve of signal vs. τ change with shimming? Does the maximum shift from $\tau = 0$ in any of the simulations? If you do a sum-of-squares combination of the shimmed signals, do you see a shift then? For simplicity, simulations in one-dimension, with a linear gradient inhomogeneity, without diffusion and completely ignoring any effect of CBV/dHb should suffice to isolate the effect of shimming/macroscopic field inhomogeneity.

   b) Alternatively, using the data on hand, consider voxels that showed a large shift parameter and compare them to voxels that had a negligible shift parameter in some of the following ways: Look at the entire "decay" curve of signal vs. τ without shimming. Is the maximum shifted from $\tau = 0$? How do these decay curves look at various shim levels? Does the maximum shift? What happens to the signal at $\tau = 0$ with shimming? Does the signal for $\tau \neq 0$ actually exceed the signal at $\tau = 0$ (unshimmed) for some shimming value?

   c) Again using the experimental data, is the shift something like a fitting artifact? For voxels with large ΔT, are the decay curves vs. τ steep or shallow (relative to the peak intensity at ΔT)? If shallow, i.e., R2' is small, then could the peak shift be the result of trying to fit a peak to a relatively flat curve + noise? Is there some correlation between R2' and ΔT that may support this?

Minor Comment:
In the Imaging Protocol subsection of the Methods, the authors state, "For the ASE sequence we modified the manufacturer's spin-echo EPI sequence to allow the 180° refocusing pulse to be offset by τ as defined above." Is the refocusing pulse offset by τ or $\tau/2$ (resulting in shifts of the echo of 2τ or τ, respectively)?

Competing Interests: No competing interests were disclosed.

Reviewer Expertise: biophysical modelling of the blood oxygenation level-dependent (BOLD) fMRI signal, high-resolution fMRI, MRI pulse sequence development

I confirm that I have read this submission and believe that I have an appropriate level of expertise to confirm that it is of an acceptable scientific standard, however I have significant reservations, as outlined above.

Author Response 04 Aug 2022

Tobias C. Wood, Institute of Psychiatry, Psychology & Neuroscience, King's College London, UK

We thank the reviewer for their further comments.

Minor Comment: The shift of tau/2 is correctly defined in the Theory section. The manuscript has been edited to make this clearer.

Point 2: The acquired signal can be greater than at the spin echo in the presence of Macroscopic Field Gradients. This is the reason Z-shimming was proposed for OEF mapping by Blockley et al. Investigations as proposed in (b) were performed during study setup and led to the idea of adding the shift parameter. There are no obvious correlations as suggested in (c), which can be seen visually in figure 4 (the shift parameter has a different spatial pattern to R2'). The decay curves are indeed fairly flat and noisy, we have already included discussion of the trade-offs that would be involved in better estimation of R2' - "We hypothesise that adjusting the protocol to acquire fewer intermediate values of τ and additional images with high values and near $\tau=0$ could improve the sensitivity to both DBV and R2'[58]. Increasing the maximum value of τ would necessitate either a corresponding increase in TE, which would reduce SNR and increase the effects of MFGs[19], or the use of Partial Fourier acceleration, which we found caused unacceptable blurring and intensity artefacts from the echo moving out of the EPI acquisition window[30]". The investigations suggested in (a) would be significant extra work that is beyond the scope of this manuscript. We have investigated the fitting of our data as thoroughly as we consider reasonable, and further investigations are beyond the scope of this work. We have now added the raw data to the downloadable data, which will allow interested parties to conduct additional investigations if they so choose.

Competing Interests: No competing interests were disclosed.

Version 2

Reviewer Report 24 January 2022

✔ **Yolanda Ohene** (iD)

The University of Manchester, Manchester, UK

No further comments.

Competing Interests: No competing interests were disclosed.

Reviewer Expertise: MRI - Arterial Spin Labelling

I confirm that I have read this submission and believe that I have an appropriate level of expertise to confirm that it is of an acceptable scientific standard.

Reviewer Report 11 October 2021

https://doi.org/10.21956/wellcomeopenres.18968.r45803

? **Avery Berman** (iD)

[1] Athinoula A. Martinos Center for Biomedical Imaging, Massachusetts General Hospital, Charlestown, MA, USA
[2] Department of Physics, Carleton University, Ottawa, ON, Canada
[3] Brain Imaging Centre, The Royal Ottawa Institute of Mental Health Research, Ottawa, ON, Canada

Wood *et al.* have updated their manuscript to help address most of my previous concerns and those of Reviewer 1. I would like to thank the authors for adding some key references from the literature. I still have reservations for my original comments 1 and 2.

The authors have referenced the paper by Miller and Joseph (1993) regarding the validity of the noise floor correction on relaxometry (my original comment 1). The noise floor correction from Miller and Joseph was specifically for the root-sum-of-squares (RSS) combination of single-channel real and imaginary data. Here, the authors have combined images from multiple z-shims (>2) which themselves are the result of RSS combination of 4-channel data. A different correction factor may be required for 4-channel data, although it's not immediately obvious to me how this then applies to the combination of multiple z-shimmed images (perhaps they can be treated as additional channels). Koay and Basser (2006, J Magn Reson)[1] have examined this correction factor for multi-channel RSS (see also a follow-up paper from Bai *et al.* [2014, J Magn Reson]).[2]

Regarding the R_2' fitting parameter ΔT, which was introduced in the original manuscript to account for shifts in the signal maximum away from the nominal spin-echo image at τ = 0. This was comment 2 in my previous review. In their response, the authors have suggested that this could be due to large macroscopic field inhomogeneity along the non-shimmed direction (x-axis). I am still not convinced that this is the source of the shift since the whole point of the refocusing pulse is to refocus dephasing that arises from these static field inhomogeneities at the spin-echo. The reference that was added from Chen et al., was specifically discussing gradient-echo, and its relevance to asymmetric spin-echo was mentioned; however, their theory does not apply to the spin-echo. I think there are multiple ways one could go about investigating the nature of this shift with the data on hand or with some straightforward modelling. This may not, in the end, affect the fitted R_2' values, but I think it would go a long way to help solidify the methodological underpinnings of the proposed R_2'/OEF mapping.

References
1. Koay CG, Basser PJ: Analytically exact correction scheme for signal extraction from noisy magnitude MR signals. *J Magn Reson*. 2006; **179** (2): 317-22 PubMed Abstract | Publisher Full Text
2. Bai R, Koay CG, Hutchinson E, Basser PJ: A framework for accurate determination of the T_2 distribution from multiple echo magnitude MRI images. *J Magn Reson*. 2014; **244**: 53-63 PubMed Abstract | Publisher Full Text

Competing Interests: No competing interests were disclosed.

Reviewer Expertise: biophysical modelling of the blood oxygenation level-dependent (BOLD) fMRI signal, high-resolution fMRI, MRI pulse sequence development

I confirm that I have read this submission and believe that I have an appropriate level of expertise to confirm that it is of an acceptable scientific standard, however I have significant reservations, as outlined above.

Author Response 08 Dec 2021

Tobias C. Wood, Institute of Psychiatry, Psychology & Neuroscience, King's College London, UK

We thank the reviewer for their further comments.
1. The reviewer did not raise the issue of the multi-channel combination or provide these references in their first review. This topic is far beyond the scope of the paper. The principal reason for the noise correction was to remove background noise, as described in the caption of figure 3, such that processing steps such as brain extraction and registration could be achieved. The low echo-offset that we could achieve means that within the brain there is not a large amount of signal decay, i.e. within the brain we appear to be operating in a reasonable SNR regime, and we do not reach the noise floor of T2' decay.

2. The introduction of the shift parameter was the most straightforward, empirical way to address the issue. As can be seen in figure 4 the resulting value of the shift parameter is close to zero over most of the brain including the cortex. It is hence not

the source of the R2' prime underestimation we observed, which occurred over the whole brain, and is by far the more important issue which we have now dedicated significant space to discussing. The reviewer suggests in his reply that there are multiple ways to investigate the nature of the T2' shift but a list of such ways is missing, hence it is not possible to respond further to this comment.

Competing Interests: No competing interests were disclosed.

- -

Version 1

Reviewer Report 04 June 2021

https://doi.org/10.21956/wellcomeopenres.18455.r43881

✔

Yolanda Ohene 🆔

The University of Manchester, Manchester, UK

Wood *et al*. have combined two techniques, arterial spin labelling (ASL) and asymmetric spin-echo (ASE), that capture the cerebral blood flow (CBF) and the oxygen extraction fraction (OEF), respectively, to provide a non-invasive measurement of cerebral metabolic rate of oxygen ($CMRO_2$).

$CMRO_2$ measurements were taken in rodents under two different anaesthetic conditions. The authors demonstrate that $CMRO_2$ is lower under α-Chloralose anaesthesia compared to isoflurane anaesthesia. The metabolic activity was validated by measuring glucose consumption using autoradiography under the same two anaesthetic conditions. The glucose metabolic rate is also lower under α-Chloralose anaesthesia. The study design resulted in a clear separation of the OEF, CBF, $CMRO_2$ and glucose utilisation (GU) under the two anaesthetic conditions, in almost all brain regions, demonstrating the successful implementation of this non-invasive method.

Minor comments:
- Could the authors comment on the effect of fixing the deoxygenated blood volume (DBV) in the OEF measurements, particularly considering that there is a significant difference in the CBF between the two anaesthesia groups which may have an influence on the DBV value?

- Introduction, Paragraph 1: Typo – "Bloody" to "Blood".

- Figure 5: Labelling of the coloured bars are overlapping on the bottom row images.

Is the rationale for developing the new method (or application) clearly explained?
Yes

Is the description of the method technically sound?
Yes

Are sufficient details provided to allow replication of the method development and its use by others?
Yes

If any results are presented, are all the source data underlying the results available to ensure full reproducibility?
Yes

Are the conclusions about the method and its performance adequately supported by the findings presented in the article?
Yes

Competing Interests: No competing interests were disclosed.

Reviewer Expertise: MRI - Arterial Spin Labelling

I confirm that I have read this submission and believe that I have an appropriate level of expertise to confirm that it is of an acceptable scientific standard.

Author Response 22 Oct 2021
Tobias C. Wood, Institute of Psychiatry, Psychology & Neuroscience, King's College London, UK

We thank the reviewer for their further comments.
1. The reviewer did not raise the issue of the multi-channel combination or provide these references in their first review. This topic is far beyond the scope of the paper. The principal reason for the noise correction was to remove background noise, as described in the caption of figure 3, such that processing steps such as brain extraction and registration could be achieved. The low echo-offset that we could achieve means that within the brain there is not a large amount of signal decay, i.e. within the brain we appear to be operating in a reasonable SNR regime, and we do not reach the noise floor of T2' decay.

2. The introduction of the shift parameter was the most straightforward, empirical way to address the issue. As can be seen in figure 4 the resulting value of the shift parameter is close to zero over most of the brain including the cortex. It is hence not the source of the R2' prime underestimation we observed, which occurred over the whole brain, and is by far the more important issue which we have now dedicated significant space to discussing. The reviewer suggests in his reply that there are multiple ways to investigate the nature of the T2' shift but a list of such ways is

> missing, hence it is not possible to respond further to this comment.
>
>
> **Competing Interests:** No competing interests were disclosed.

Reviewer Report 02 June 2021

https://doi.org/10.21956/wellcomeopenres.18455.r43877

? **Avery Berman** (iD)
[1] Athinoula A. Martinos Center for Biomedical Imaging, Massachusetts General Hospital, Charlestown, MA, USA
[2] Department of Physics, Carleton University, Ottawa, ON, Canada
[3] Brain Imaging Centre, The Royal Ottawa Institute of Mental Health Research, Ottawa, ON, Canada

Wood *et al.* have presented a new R_2'-based method for quantifying the oxygen extraction fraction (OEF) and the cerebral metabolic rate of O_2 (CMRO$_2$) in rats. The novelty here lies in i) the variable shimming approach used to reduce the effect of macroscopic field inhomogeneities that otherwise contaminate the contribution to R_2' from deoxyhemoglobin in the vasculature, ii) the application of this approach to compare various brain physiological parameters (OEF, CBF, CMRO$_2$) under two different anesthetics (isoflurane and alpha-Chloralose) and iii) the comparison of CMRO$_2$ to the glucose uptake (GU) by autoradiography.

The study shows large differences in brain physiology under the different anesthetics, consistent with previous findings. The final finding that the authors fit a CMRO$_2$ to GU ratio of 6.4 is quite remarkable, considering the theoretical ratio is 6 (i.e., 6 molecules of O_2 consumed per glucose during oxidative glycolysis). I do have significant concerns, however, with the quantification of R_2' given that multiple previously unpublished techniques were employed that I think would benefit from further validation. Given that the OEF and CMRO$_2$ quantification rely on the estimate of R_2', this does have important consequences for the comparisons of the absolute OEF and CMRO$_2$ values across the two anesthetics and for the absolute CMRO$_2$:GU ratio.

1. To the best of my knowledge, the way the shimmed images were combined through root sum of squares is a previously unpublished approach. Similarly, the proposed noise floor correction via subtraction of the mean-squared noise signal in the background is also novel to this study. While the noise subtraction does appear to improve the contrast-to-noise, it is not apparent that the desired absolute signal levels are preserved. Since these images are later used for absolute quantification of R_2', it is important that the signal levels are not systematically biased, but if they are, at least that bias can be characterized. It would be reassuring to see a validation of these new techniques.

2. The authors introduced the R_2' fitting parameter ΔT to account for shifts in the signal maximum away from the nominal spin-echo time at τ = 0. The magnitude of the shifts, ±25 ms, are dramatic and are previously unheard of (to the best of my knowledge). This is possibly related to the shimming and/or the shim image combination. Again, some form of external validation of this parameter to better understand its origin would help give better trust in the resulting R_2' fits.

3. Another major limitation of this study was that the R_2' fitting required fixing the value of deoxygenated blood volume (DBV) to 3.3%. While this may have helped stabilize the fit, it would lead to OEF estimates that would differ from their true values depending on how the true DBV compared to the assumed value, and this points to issues with the model and/or data. As DBV is regionally varying, this limits the validity of the OEF estimates. Could the authors elaborate on how they performed the fitting? In Eq. 2, there is the quadratic decay period for tau < Tc and the linear decay period for tau > Tc. Also note, typically studies have used a factor of 1.5*Tc for the transition period, although this would depend on how the authors have defined Tc (e.g, refs. 17 or 19). Was data from all periods fit? How was Tc determined without a priori knowing R_2'? In previous quantitative BOLD studies, the linear decay period is extrapolated to the signal at tau = 0 and the difference between this signal and the measured signal is proportional to DBV, was this fitting approach used here?

Minor comments:
1. In the opening paragraph, the authors refer to "quantitative BOLD" using calibration with gases. This calibration with gases is referred to as "calibrated" BOLD or fMRI, not quantitative BOLD. Quantitative BOLD is a gas-free technique which the methods in this manuscript are based on.

2. The values for the arterial O_2 concentration, Ca, are based on human physiological parameters. The authors should consider using values for rats. See, e.g., Gagnon *et al.*, J Neurosci (2015).[1]

3. The labels are cropped in Figure 5

4. In the middle of the Discussion section, the authors compare their OEF estimates to He *et al.*'s where they state findings that were in line with the findings of this manuscript. I think that stating the results being in line with each other is a bit generous as the OEF values in the manuscript differ by 35% (iso.) and 44% (alpha-chlor.) relative to those from He et al.

5. It would be nice to see a discussion of other contributions to R_2' contamination beyond macroscopic field inhomogeneities, such as iron depositions or regionally varying myelination since these may also bias the OEF estimate and would be important to be aware of in (pre)clinical studies.

6. It would be helpful to label some of the key ROIs discussed in the manuscript, in particular the inferior colliculus.

References
1. Gagnon L, Sakadžić S, Lesage F, Musacchia JJ, et al.: Quantifying the microvascular origin of

BOLD-fMRI from first principles with two-photon microscopy and an oxygen-sensitive nanoprobe.*J Neurosci*. 2015; **35** (8): 3663-75 PubMed Abstract | Publisher Full Text

Is the rationale for developing the new method (or application) clearly explained?
Yes

Is the description of the method technically sound?
Partly

Are sufficient details provided to allow replication of the method development and its use by others?
Partly

If any results are presented, are all the source data underlying the results available to ensure full reproducibility?
Yes

Are the conclusions about the method and its performance adequately supported by the findings presented in the article?
Partly

Competing Interests: No competing interests were disclosed.

Reviewer Expertise: biophysical modelling of the blood oxygenation level-dependent (BOLD) fMRI signal, high-resolution fMRI, MRI pulse sequence development

I confirm that I have read this submission and believe that I have an appropriate level of expertise to confirm that it is of an acceptable scientific standard, however I have significant reservations, as outlined above.

Author Response 09 Sep 2021

Tobias C. Wood, Institute of Psychiatry, Psychology & Neuroscience, King's College London, UK

We thank the reviewer for their constructive feedback. Responses to the individual points are below.

Major:

1. A key reference describing the use of the root-sum-squares method for combining z-shimmed images (Spencer & Constable 1999) was omitted. This has now been corrected. Similarly, the noise floor correction method has also been previously published (Miller & Joseph 1993, reference 40) where it was used in the context of T2/R2 fitting. While these techniques are old to our knowledge they have not been invalidated.
2. We agree with the reviewer that such shifts have not been described previously in the

literature, however the linear extrapolation method used by Blockley et al cannot detect such shifts even if they are present. In addition, previous literature in this area has used human subjects and lower field strengths. We suspect that strong MFGs in the x-direction, which we could not compensate due to scan time constraints, may be the underlying cause of such shifts. This putative explanation has been added to the discussion, along with an additional reference (Chen et al)

3. We agree that fixing the value of DBV is a limitation of this study. We previously used a value of 1.5Tc for the transition period and Tc=R2'/DBV and a non-linear fit across all data points. Whave now updated the code (and relevant equations in the manuscript) to use the full integral form of Yablonskiy et al, but note that this made very little difference to the fitted values compared to the asymptotic form of the equations. This code is now available in version 3.3 of our toolbox. Likely, a major contributor to the difficulty in fitting for DBV is the relatively small maximum value of τ we could achieve within imaging constraints and only having a single τ=0 image. A more efficient protocol may be to acquire multiple τ=0 images and fewer intermediate values of τ. This point has been expanded in the discussion.

Minor comments:

1. Thank you for the clarification, the introduction has been reworded accordingly.

2. We thank the reviewer for bringing this to our attention. Please see the notes on the amendments at the start of the text for a full discussion of this issue.

3. The labels have been corrected in figure 5.

4. On reflection we agree with the reviewer. The sentence has been amended to state that the values in He et al are further evidence that our method currently underestimates OEF.

5. Discussion of the effect of myelination has been added, as it is clear the current model does not account for this.

6. Due to the 3D nature of the ROIs, displaying all of them would require an additional figure. The Inferior Colliculus has been marked on an existing figure with arrows.

Competing Interests: No competing interests were disclosed.